Single-cell analysis of severe COVID-19 patients reveals a monocyte-driven inflammatory storm attenuated by Tocilizumab

Chuang Guo[1,7], Bin Li[1,7], Huan Ma[1], Xiaofang Wang[2], Pengfei Cai[1], Qiaoni Yu[1], Lin Zhu[1], Liying Jin[1], Chen Jiang[1], Jingwen Fang[3], Qian Liu[1], Dandan Zong[1], Wen Zhang[1], Yichen Lu[1], Kun Li[1], Xuyuan Gao[1], Binqing Fu[1,4], Lianxin Liu[2], Xiaoling Ma[5], Jianping Weng[6], Haiming Wei[1,4], Tengchuan Jin[1,4,†], Jun Lin[1,4,†], Kun Qu[1,4,†]

[1]Department of oncology, The First Affiliated Hospital of USTC, Division of Molecular Medicine, Hefei National Laboratory for Physical Sciences at Microscale, Division of Life Sciences and Medicine, University of Science and Technology of China, Hefei, Anhui, 230021, China.
[2]Department of Hepatobiliary Surgery, the First Affiliated Hospital of USTC, Division of Life Sciences and Medicine, University of Science and Technology of China, Hefei, Anhui, 230021, China.
[3]HanGene Biotech, Xiaoshan Innovation Polis, Hangzhou, Zhejiang, 311200, China.
[4]CAS Center for Excellence in Molecular Cell Sciences, the CAS Key Laboratory of Innate Immunity and Chronic Disease, University of Science and Technology of China, Hefei, Anhui, 230027, China.
[5]Department of Laboratory Medicine, The First Affiliated Hospital of USTC, Division of Life Sciences and Medicine, University of Science and Technology of China, Hefei, Anhui, 230001, China.
[6]Department of Endocrinology and Metabolism, The First Affiliated Hospital of USTC, Division of Life Sciences of Medicine, University of Science and Technology of China, Hefei 230026, China.
[7]These authors contributed equally to this work.
†Corresponding should be addressed to Kun Qu (qukun@ustc.edu.cn).
Jun Lin (linjun7@ustc.edu.cn); Tengchuan Jin (jint@ustc.edu.cn)

Contact Information:

Kun Qu, Ph.D.
Division of Molecular Medicine, Hefei National Laboratory for Physical Sciences at Microscale, Division of Life Sciences and Medicine, University of Science and Technology of China, Hefei, Anhui, 230027, China.
Email: qukun@ustc.edu.cn
Phone: +86-551-63606257

ABSTRACT

Despite the current devastation of the COVID-19 pandemic, several recent studies have suggested that the immunosuppressive drug Tocilizumab can powerfully treating inflammatory responses that occur in this disease. Here, by employing single-cell analysis of the immune cell composition of severe-stage COVID-19 patients and these same patients in post Tocilizumab-treatment remission, we have identified a monocyte subpopulation specific to severe disease that contributes to inflammatory storms in COVID-19 patients. Although Tocilizumab treatment attenuated the strong inflammatory immune response, we found that immune cells including plasma B cells and $CD8^+$ T cells still exhibited an intense humoral and cell-mediated anti-virus immune response in COVID-19 patients after Tocilizumab treatment. Thus, in addition to providing a rich, very high-resolution data resource about the immune cell distribution at multiple stages of the COVID-19 disease, our work both helps explain Tocilizumab's powerful therapeutic effects and defines a large number of potential new drug targets related to inflammatory storms.

Keywords : Coronavirus disease 2019 (COVID-19); Severe acute respiratory syndrome coronavirus 2 (SARS-CoV-2); Tocilizumab; Single-cell RNA sequencing (scRNA-seq); Inflammatory storm; Monocyte

Introduction

As of May 1, 2020, the WHO has reported 224,172 deaths out of 3,175,207 confirmed cases for infection by severe acute respiratory syndrome coronavirus 2 (SARS-CoV-2), and these numbers are still growing rapidly[1]. Approximately 14% of patients with COVID-19 experienced severe disease, and 5% were critically ill, among which there was a 49% fatality rate[2]; it has been speculated that this high mortality is related to abnormal immune system activation[3, 4, 5]. Hence, there is an urgent need for researchers to understand how the immune system responds to SARS-CoV-2 viral infection at the severe stage, which may highlight potential effective treatment strategies.

Studies have shown that the inflammatory storm caused by excessive immune responses was strongly associated with mortality in COVID-19[6, 7]. Plasma concentrations of a series of inflammatory cytokines, such as granulocyte-macrophage colony-stimulating factor (GM-CSF), interleukin (IL)-6[4], tumor necrosis factor α (TNF-α), IL-2, 7, 10, and granulocyte colony-stimulating factor (G-CSF)[8] were increased after SARS-CoV-2 infections. Further investigation demonstrated that peripheral inflammatory monocytes and pathogenic T cells may incite cytokine storm in severe COVID-19 patients[4, 6]. Tocilizumab, an immunosuppressive drug that targets IL-6 receptors, has been used to treat severe COVID-19 patients[9, 10], as it is effective for treating severe and even life-threatening cytokine-release syndrome [11, 12]. After receiving Tocilizumab, the body temperature of the patients returned to normal after 24 hours, and Tocilizumab was shown to significantly decrease the concentration of oxygen inhalation by COVID-19 patients by the 5th day of treatment[13]. Despite the apparent efficacy of Tocilizumab for treating severe COVID-19 patients, the lack of single-cell level analyses has prevented any deepening of our understanding about how Tocilizumab impacts the typical COVID-19 induced activation of an inflammatory storm.

In the present study, we profiled the single-cell transcriptomes of 13,239 peripheral blood mononuclear cells (PBMCs) isolated at the severe and remission

disease stages of two severe COVID-19 patients treated with Tocilizumab. We identified a severe-stage-specific monocyte subpopulation that clearly contributes to the patients' inflammatory storms. Comparison between the severe and remission disease stages at the single-cell level revealed that Tocilizumab treatment weakens the excessively activated inflammatory immune response and also showed that immune cells, including plasma B cells and $CD8^+$ T cells, still exhibit boosted humoral and cell-mediated anti-virus immune responses in post-treatment COVID-19 patients. Our study thus provides a rich, high-resolution data set about the immune context at multiple stages of COVID-19, and helps to explain how a promising candidate drug both alters immune cell populations and reduces patient mortality.

Results

An atlas of peripheral immune cells in severe COVID-19 patients

We obtained 5 peripheral blood samples from 2 severe COVID-19 patients at 3 time points including the severe and remission stages during Tocilizumab treatment (Fig. 1a). Specifically, we collected blood samples at day 1— within 12 hours of Tocilizumab administration—and at day 5 for both patients; note that we also obtained a blood sample from patient P2 on day 7 of Tocilizumab treatment because P2 still had a positive result for a SARS-Cov-2 nucleic acid test of a throat swab specimen on day 5. At day 1, the patients both had a decreased number of lymphocytes compared to healthy reference interval, as well as increased percentages of neutrophils and elevated concentrations of C-reaction protein and increased expression of IL-6 (Supplementary Table 1). Since the clinical symptoms of most of the severe COVID-19 patients, including both patients in this study, were remarkably improved by 5 days of Tocilizumab treatment[13] (Supplementary Table 1), we defined the blood draws from day 5 as the "remission stage". For patient P2, we took another blood draw at day 7, when his nucleic acid test turned negative (Fig. 1a). It is worth noting that patient P1 was discharged on day 8, and patient P2 on day10, and these

discharges were both at 3 days after a nucleic acid test of a throat swab specimen was negative.

We isolated the PBMCs from the COVID-19 patients' blood samples and subjected them to single-cell mRNA sequencing (scRNA-seq) using the 10X platform (Fig. 1a). After rigorous quality control definition (Supplementary Fig. 1a-d, Supplementary Table 2), low quality cells were filtered; we also removed cell doublets using Scrublet[14]. Correlation of the gene expression for the samples from either patient emphasized the excellent reproducibility between the technical and biological replicates of our dataset (Supplementary Fig. 1e-f). After quality control (QC) and doublet removal, our dataset comprised a total of 13,239 high-quality transcriptomes for single PBMCs.

Due to the similarities between the single-cell transcriptomes of most of the identified cell subsets at the severe and remission disease stages, we initially combined the samples from both patients from day 1 as the "severe stage" and combined the samples from day 5 (and day 7 for P2) as the "remission stage"; note that we also conducted separate analyses for each patient, which yielded similar data trends (Supplementary Fig. 2a, b). In total, the combined analyses of all the single-cell transcriptomes for the COVID-19 patients included 4,344 cells from the severe disease stage and 8,895 were from the remission disease stage.

To investigate heterogeneity among the PBMCs for the COVID-19 patients compared to healthy controls, we applied Seurat[15] (version 3.1.4) to integrate our COVID-19 single-cell transcriptomes with the published single-cell profiles of healthy PBMCs from the 10X official website[16], enabling an analysis with a total of 68,190 cells (See **Methods**). We then normalized and clustered the gene expression matrix; this identified 18 unique cell subsets, which were visualized via uniform manifold approximation and projection (UMAP) (Fig. 1b-d). Cell lineages, including monocytes, $CD4^+$ and $CD8^+$ T, γδT, natural killer (NK), B, plasma B and myeloid dendritic cells (mDC), plasmacytoid dendritic cells (pDC), platelets, and $CD34^+$

progenitor cells were identified based on the expression of known marker genes (Fig. 1e). This analysis represents a delineation of the landscape of circulating immune cells for severe COVID-19 patients.

We also used another integration method, Harmony[17], to help assess the accuracy of the cell clustering results from Seurat[15] (version 3.1.4) and again visualized the results in UMAP (Supplementary Fig. 3a). We found strong correlations for the identified cell subsets and the detected gene expression patterns between the cell clusters with the two integration methods (Supplementary Fig. 3b, c), supporting the robustness of our cell clustering results.

We next explored the distribution of immune cells from the severe and remission stage COVID-19 patients, as well as in healthy control individuals (Supplementary Fig. 4a). We observed that a number of subpopulations, such as pDCs (cluster 15), mDCs (cluster 10), and most monocytes (clusters 2 and 13) were present in remission stage COVID-19 patients and in healthy controls but not in severe COVID-19 patients (Supplementary Fig. 4b), indicating that Tocilizumab treatment gradually restores a normal distribution of these cell types in circulating blood. Some cell subsets such as NK cells (cluster 7) and $CD4^+$ T cells (cluster 1 and 4) were quite heterogeneous between the two COVID-19 patients, so we did not examine these cell types further. These analyses revealed the conspicuous presence of four cell populations that were uniquely present in the COVID-19 patients (albeit to differencing extents in the severe vs. remission disease stages), including a monocyte subpopulation (cluster 9), plasma B cells (cluster 11), effector $CD8^+$ T cells (cluster 6), and proliferative $MKI67^+CD8^+$ T cells (cluster 12) patients (Supplementary Fig. 4c). Given our study's aim of characterizing the COVID-19-specific and Tocilizumab-sensitive immune cell populations of COVID-19 patients, the majority of our subsequent detailed analyses focused on these four cell populations.

A monocyte subpopulation contributes the inflammatory storm in severe stage

177 **COVID-19 patients**

178 Monocytes have been reported to play a vital role in CAR-T induced
179 cytokine-release syndrome[18] and in SARS-CoV-2 infection triggered inflammatory
180 storms[4], so we explored the features and functions of the aforementioned monocyte
181 subpopulation that we detected in our single-cell analysis of the two COVID-19
182 patients. We detected 1,677 monocytes in patients, with 916 from the severe disease
183 stage and 761 from the remission stage; we examined these alongside the data for
184 9,517 monocytes from health controls. The UMAP plot displayed two main clouds of
185 monocytes that were clearly segregated (Fig. 2a). One monocyte subpopulation
186 (cluster 9) consisted of 98.3% of all monocytes at severe stage, while this ratio was
187 only 12.1% at remission stage and 0% in healthy controls (Fig. 2b), so we initially
188 assessed these severe-stage-specific monocytes.

189 Transcriptional differences among monocytes subtypes was detected based on a
190 pairwise comparison of the gene expression in the severe and remission stages and in
191 respective comparisons against healthy control individuals. A large number of
192 differentially expressed genes (DEGs) with reported inflammation-related functions
193 were observed in the severe-stage-specific monocytes, including the previously
194 reported cytokine-storm-related genes such as *TNF*[8], *IL10*[8], *CCL3*[8], and *IL6*[4];
195 inflammatory related chemokine genes *CCL4*, *CCL20*, *CXCL2*, *CXCL3*, *CCL3L1*,
196 *CCL4L2*, *CXCL8* and *CXCL9*; and inflammasome activation associated genes *NLRP3*
197 and *IL1B* in the severe-stage-specific monocytes (Fig. 2c, fold change > 2, $P < 10^{-3}$,
198 Wilcoxon rank-sum test; Fig. 2d; and Supplementary Table 3). Collectively, the large
199 number of DEGs with reported inflammation-related functions support the idea that
200 the severe-stage-specific monocyte subpopulation we detected in our single-cell
201 COVID-19 patient data may strongly support development of inflammatory responses
202 in severe COVID-19 patients.

203 A GO analysis indicated enrichment of genes with annotations related to
204 “regulation of acute inflammatory response” , “regulation of leukocyte activation”,

"cell chemotaxis" and "cellular response to chemokine" in severe-stage COVID-19 patients compared to remission-stage patients and healthy controls (Fig. 2e, f, $P < 10^{-117}$, Wilcoxon rank-sum test; Supplementary Fig. 5; and Supplementary Table 4, 5), suggesting that the inflammatory storm caused by this monocyte subpopulation is suppressed by Tocilizumab treatment.

Next, we explored transcription factors (TFs) in monocytes which may be involved in the promoting of the inflammatory storm. We used SCENIC[19] and predicted 9 TFs that may regulate genes that were up-regulated in severe-stage-specific monocytes (Fig. 2g). We then constructed a gene regulatory network among the SCENIC predicted TFs and a set of inflammation-relevant genes that were collected from the literatures [20, 21]. We found that 3 of the SCENIC predicted TFs, namely *ATF3*, *NFIL3*, and *HIVEP2*, may have the capacity to regulate the detected inflammation-relevant genes (Supplementary Fig. 6). Additionally, we found that the expression of *ATF3*, *NFIL3*, and *HIVEP2* and their motif enrichment which was predicted by the expressing of their potential target genes were enhanced in the severe-stage-specific monocyte subpopulation (Fig. 2h), further supporting that these 3 TFs may regulate the observed inflammatory storm in monocytes.

Recent studies have shown that over 20% of the severe COVID-19 patients had symptoms of severe septic shock, which affects several organ systems and contributes to liver injury[22], acute kidney failure[23], and abnormal heart damage[24]. We therefore checked whether this severe-stage-specific monocyte subpopulation is unique to COVID-19. We downloaded scRNA-seq datasets from patients with sepsis at a mild stage (Int-URO) and patients with sepsis at a severe stage (ICU-SEP), as well as critically ill patients without sepsis (ICU-NoSEP) and healthy controls (Control)[25]. We then integrated these data sets with our COVID-19 patients' single-cell data using Seurat[15] (version 3.1.4), which revealed a total of 10 monocyte cell clusters (Supplementary Fig. 7a, b). Interestingly, the cells from the severe stage COVID-19 patients clearly overlapped with only one of the integrated monocyte clusters (cluster

VI) (Supplementary Fig. 7c), suggesting that the severe-stage-specific monocyte population might be unique to COVID-19.

A monocyte-centric cytokine/receptor interaction network in severe-stage COVID-19 patients

Given that monocytes in the severe stage may be involved in the regulation of a variety of immune cell types, we used the accumulated ligand/receptor interaction database[26] CellPhoneDB (www.cellphonedb.org) to identify alterations of molecular interactions between monocytes and all of the immune cell subsets we identified in our single-cell analysis (Supplementary Table 6). We found 15 cytokine/receptors pairs whose interactions were significantly boosted in severe-stage COVID-19 patients as compared to remission stage patients and healthy controls (Fig. 3a). It is notable that the expression of multiple inflammatory-storm-related cytokines/receptors was significantly increased in severe stage COVID-19 patients (Fig. 3b), which seems plausible that monocytes may have a substantially increased propensity for interaction with other immune cells in blood vessels. Our comparison between severe stage and remission stage patients also suggested obvious attenuation of increased cytokine/receptor interaction activity among the immune cells of remission COVID-19 patients (Fig. 3b). While clearly preliminary, our data support a role for Tocilizumab in reducing monocyte receptor compositions that have been previously implicated in the induction of inflammatory storms.

Consistent with a previous reported that the inflammatory monocytes released IL-6 play an vital role in inciting inflammatory storm in severe COVID-19 patients[4], we found monocytes were predicted to communicate with $CD4^+$ T cells and plasma B cells at severe stage COVID-19 patients through the cytokine/receptor pairs of IL-6/IL-6R. We also detected that the severe-stage-specific monocytes featured elevated expression of other cytokine/receptor pairs that may contribute to a broad spectrum of immune cell communications, such as TNF-α and its receptors, through

which monocytes may interact with $CD4^+$ T, $CD8^+$ T and B cells. Similarly, the severe-stage monocytes had elevated levels of IL-1β and its receptor, suggesting potentially functional interaction of these monocytes with $CD8^+$ T cells. Chemokines such as CCL4L2, CCL3, and CCL4 and their respective receptors were also found to be enriched in severe stage monocytes, indicating the potential of targeting these cytokines and/or their receptors as possible drug targets for treating severe-stage COVID-19 patients. Indeed, it is notable that inhibitors targeting some of these cytokine/receptor pairs are currently undergoing anti-COVID-19 clinical trials in multiple places around the world (Supplementary Table 7). Collectively, these findings help illustrate the possible molecular basis of cell-cell interactions at the peripheral blood of COVID-19 patients, leading to a better understanding of the mechanisms of inflammatory storm of the disease.

Boosted humoral and cell-mediated immunity in severe COVID-19 patients

Studies of avian H7N9 disease have revealed that viral infection can elicit robust, multi-factorial immune responses[27, 28], and a very recent study reported effective immune responses from a non-severe COVID-19 patient[29]. However, it is not clear whether the anti-virus immune responses are affected by Tocilizumab treatment. We assessed the anti-virus immune responses—both humoral and cell-mediated immune responses—of severe-stage COVID-19 patients as compared with both remission stage patients and healthy controls. As expected for un-infected controls, there were hardly any plasma B cells in healthy individuals (Fig. 4a). In contrast, there were many plasma B cells in both the severe and remission stage COVID-19 patients (Fig. 4a, b), suggesting that SARS-CoV-2 infection may elicit the anti-virus humoral immune responses, which are not affected by the Tocilizumab treatment.

$CD8^+$ T cells are function in cell-mediated immunity against viral infections by killing infected cells and secreting proinflammatory cytokines[30]. Our single-cell analysis detected a total of 13,602 $CD8^+$ T cells. Clustering of these cells revealed 3

subtypes: naïve $CD8^+$ T cells (cluster 3), effector $CD8^+$ T cells (cluster 6), and a subset of $CD8^+$ T cells with obvious expression of known proliferation markers (cluster 12) (Fig. 4c, d). The $CD8^+$ T cells of the severe patients were primarily of the effector $CD8^+$ T cell cluster (Fig. 4c, d). We then conducted pairwise comparisons to identify DEGs in the effector $CD8^+$ T cells among the severe and remission stage patients and in healthy controls (Fig. 4e, Supplementary Table 8). A GO analysis indicated that DEGs in severe stage effector $CD8^+$ T cells exhibited enrichment for "positive regulation of cell activation" (Fig. 4f, $P < 10^{-10}$; hypergeometric test; Supplementary Table 9). Conversely, DEGs of the $CD8^+$ T cells from severe and remission stage COVID-19 patients (i.e., vs. healthy controls) were enriched for functional annotations relating to "cell chemotaxis" and "regulation of cell killing" (Fig. 4g, $P < 10^{-6}$; hypergeometric test; Supplementary Table 9). We also detected significant elevated expression of the 306 and 94 genes involved in these GO terms (Fig. 4h, i, $P < 10^{-32}$, Wilcoxon rank-sum test; Supplementary Table 10). Together, these results indicate that SARS-CoV-2 infection elicits robust adaptive immune responses and suggest that Tocilizumab treatment further promotes such responses.

To gather additional empirical support from COVID-19 patients, we downloaded the bulk RNA-seq data of PBMCs from 3 severe COVID-19 patients and 3 healthy controls[31], and applied AutoGeneS[32] to deconvolute the composition of cell clusters based on the signature genes identified in our single-cell analysis. Our results indicated that there were significantly more severe-stage-specific monocytes (cluster 9), plasma B cells (cluster 11), and proliferating $CD8^+$ T cells (cluster 12) in severe COVID-19 patients compared with healthy controls (Supplementary Fig. 8a-c, $P <$ 0.05, Student's t-test), findings consistent with our main conclusions.

Discussion

The immune system is exerts essential functions in fighting off viral infections[33, 34]. Recent studies have indicated that monocytes can exacerbate and even be a

317 primary factor in the mortality of COVID-19 by contributing to inflammatory storms[4].
318 In the present study, we used single-cell mRNA sequencing and discovered a specific
319 monocyte subpopulation that may lead to the inflammatory storm in severe-stage
320 COVID-19 patients. By analyzing the monocyte-centric cytokine/receptor
321 complements and predicting interaction networks, we uncovered a
322 severe-stage-specific landscape of peripheral immune cell communication which may
323 drive the inflammatory storm in COVID-19 patients. Our identification of this
324 monocyte subpopulation and these cytokine-storm-related cytokine/receptor provides
325 mechanistic insights about the immunopathogenesis of COVID-19 and suggests the
326 potential of these cytokine/receptor molecules as candidate drug targets for treating
327 the disease.

328 There have long been questions about whether treatment with the
329 immunosuppressive agent Tocilizumab may affect the body's antiviral responses[35, 36].
330 Our single-cell profiles illustrated a sustained humoral and cell-mediated anti-virus
331 immune response in severe and remission stage COVID-19 patients. For example,
332 Tocilizumab treatment of severe-stage COVID-19 patients retained a high proportion
333 of plasma B cells with antibody-secreting functions and we found that the cytotoxicity
334 and cytokine production of effector $CD8^+$ T cells remained stable upon Tocilizumab
335 treatment.

336 Our work represents a collaborative clinical/basic effort that does provide an
337 unprecedented empirical window for studying single-cell resolution profiles from
338 severe COVID-19 patients. Deconvolution analysis of published bulk RNA-seq data[31]
339 from 3 additional severe COVID-19 patients and healthy controls helps support our
340 conclusions on the enrichment of severe-stage-specific monocytes and plasma B cells
341 in severe-stage COVID-19 patients. We further integrated additional single-cell
342 datasets from sepsis patients and found the severe-stage-specific monocytes we
343 observed are unique to severe COVID-19. Based on the incorporation of diverse
344 additional data, our study and empirical data provide actionable insights that will help

the multiple research communities who are still fighting against the virus, including clinical physicians, drug developers, and basic scientists.

Methods

Human samples

Peripheral blood samples were obtained from two severe COVID-19 patients. The patient severity was defined by the "Diagnosis and Treatment of COVID-19 (Trial Version 6)" which was released by The General Office of the National Health Commission and the Office of the National Administration of Traditional Chinese Medicine. Patient P1 was defined as a severe patient for his peripheral capillary oxygen saturation (SPO2) <93% without nasal catheter for oxygen. Patient P2 was defined as critical ill for respiratory failure, multiple organ dysfunction (MOD) and SPO2 <93 without nasal catheter for oxygen. Two peripheral blood samples were obtained for patient P1 on day 1 and day 5, and three peripheral blood samples were obtained for patient P2 on day 1, day 5 and day 7. For both patients, peripheral blood samples of day 1 were collected within 12 hours of Tocilizumab administration, when the patients were still at severe stage. Our decision to obtain blood draws from the two patients at day 5 were guided by information from the authors of the recent study published in *PNAS* [13], which guided our decision to consider day 5 of Tocilizumab treatment as a "remission stage". For patient P2, we observed that his SARS-CoV-2 nucleic acid test of a throat swab specimen was still positive at day 5, so we took another blood draw at day 7 for P2, at point by which a throat swab specimen nucleic acid test was negative. All samples were collected from the First Affiliated Hospital of University of Science and Technology of China. Before blood draws, informed consent was obtained from each patient. Ethical approvals were obtained from the ethics committee of the First Affiliated Hospital of the University of Science and Technology of China (No. 2020-XG(H)-020).

Cell Isolation

We collected 2ml peripheral blood each time from the COVID-19 patients. Peripheral blood mononuclear cells (PBMC) were freshly isolated from the whole blood by using a density gradient centrifugation using Ficoll-Paque and cryopreserved for subsequent generation of single-cell RNA library.

Single-cell RNA-seq

We generated single-cell transcriptome library following the instructions of single-cell 3' solution v2 reagent kit (10x Genomics). Briefly, after thawing, washing and counting cells, we loaded the cell suspensions onto a chromium single-cell chip along with partitioning oil, reverse transcription (RT) reagents, and a collection of gel beads that contain 3,500,000 unique 10X Barcodes. After generation of single-cell gel bead-in-emulsions (GEMs), RT was performed using a C1000 Touch^{TM} Thermal Cycler (Bio-Rad). The amplified cDNA was purified with SPRIselect beads (Beckman Coulter). Single-cell libraries were then constructed following fragmentation, end repair, polyA-tailing, adaptor ligation, and size selection based on the manufacturer's standard parameters. Each sequencing library was generated with unique sample index. Libraries were sequenced on the Illumina NovaSeq 6000 system.

Single-cell RNA-seq data processing

The raw sequencing data of patients and health donors were processed using Cell Ranger (version 3.1.0) against the GRCh38 human reference genome with default parameters, and data from different patients and disease stages were combined by the Cell Ranger 'aggr' function. We are uploading the scRNA-seq data of PBMCs from the 2 severe COVID-19 patients to the Genome Sequence Archive at BIG Data Center and the accession number will be available upon request. We also used the scRNA-seq data of PBMCs from 2 healthy donors, which can be downloaded from

the 10X genomics official website. Firstly, we filtered low quality cells using Seurat[15] (version 3.1.4). For cells from COVID-19 patients (P1 and P2), we retained cells with detected gene numbers between 500 and 6,000 and mitochondrial unique molecular identifiers (UMIs) less than 10%. For cells from healthy donors, we retained cells with detected gene numbers between 300 and 5,000 and mitochondrial UMIs less than 10%. Subsequently we adopted Scrublet[14] (version 0.2.1) to eliminate doublets in the PBMCs from the COVID-19 patients and healthy donors. We used the default parameters for Scrublet (i.e. "min_gene_variability_pctl=85, n_prin_comps=30, threshold=0.25") and detected 50 doublets from the patients and 997 doublets from the healthy donors. After removing the doublets, we normalized gene counts for each cell using the "NormalizeData" function of Seurat with default parameters.

In downstream data processing, we used canonical correlation analysis and the top 40 canonical components to find the "anchor" cells between patients and healthy controls. We then used the "IntegrateData" function in Seurat to integrate cells from COVID-19 patients and healthy controls. We clustered all the cells based on the integrated gene expression matrix using Seurat with parameter "resolution=0.3" and generated 20 clusters. To display cells in a 2-dimensional space, we ran the principal component analysis on the integrated dataset and adopted the first 50 principal components (PCs) for the uniform manifold approximation and projection (UMAP) analysis.

In the integration of cells from COVID-19 and sepsis patients using Seurat, we applied the same functions and parameters as described above. We adopted Seurat to cluster the integrated gene expression matrix (with resolution = 0.3) and identified monocyte clusters based on the expression of known marker genes *CD14* and *CD68*. We then extracted all the monocytes from the integrated dataset and re-clustered them. Finally, we generated 10 cell clusters.

Integration of cells from patients and healthy controls by Harmony

To verify the reliability of the integration results obtained using Seurat (version 3.1.4), we also applied Harmony[17] to integrate the PBMCs from COVID-19 patients and healthy controls. We used the same gene expression matrix and applied the same parameters as Seurat, and adopted the first 50 PCs to perform the data integration by calling the "RunHarmony" function in Harmony. We then used the same clustering algorithm as Seurat to cluster cells and generated 23 clusters ("resolution=0.5") based on the integration results obtained from Harmony. Jaccard index was applied to gauge the similarity between the cell clusters, with cell integration processed by Seurat or by Harmony. The Jaccard similarity between each pair of Seurat cluster (cluster *i*) and Harmony cluster (cluster *j*) were difined as follows

$$\text{Jaccard similarity} = \frac{(cells\ in\ cluster\ i) \cap (cells\ in\ cluster\ j)}{(cells\ in\ cluster\ i) \cup (cells\ in\ cluster\ j)}.$$

Differential expression analysis

To search for the differentially expressed genes (DEGs), we first assign the negative elements in the integrated expression matrix to zero. We used Wilcoxon rank-sum test to search for the DEGs between each pair of the 3 stages of cells (i.e. severe stage, remission stage and healthy control). We applied multiple thresholds to screen for DEGs, including mean fold change >2, *P* value <0.001, and were detected in >10% of cells in at least one stage.

We defined stage A specific-DEGs as the intersections between the DEGs in stage A versus stage B and the DEGs in stage A versus stage C. We defined stage A and B common-DEGs as the intersections of the DEGs in stage A versus stage C and the DEGs in the stage B versus stage C, minus the DEGs between stage A and B. In this way, we obtained the specific-DEGs for each stage, and the common-DEGs for each pair of the 3 stages. We then uploaded these DEG groups to the Metascape[37] website (https://metascape.org/gp/index.html#/main/step1), and used the default parameters to perform Gene Ontology (GO) analysis for each stage.

Motif enrichment and regulatory network

We adopted SCENIC[19] (version 1.1.2) and RcisTarget database to build the gene regulatory network of $CD14^+$ monocytes. Since the number of $CD14^+$ monocytes from healthy control (N = 9,618) was more than those from the severe and remission stages (N = 1,607), to balance their contributions in the motif analysis, we randomly sampled 2,000 $CD14^+$ monocytes from the healthy control for calculation. We selected 13,344 genes that were detected in at least 100 monocytes or included in the DEGs of the 3 stages as the input features for SCENIC. With default parameters, SCENIC generated the enrichment scores of 427 motifs. We used the student's t-test to calculate the *P* values of these motifs between severe stage and healthy control, and selected severe-specific enriched motifs with fold change >1.5 and *P* value < 10^{-100}.

We then applied the enrichment scores of the severe-specific enriched motifs and the expression of their targeted genes to Cytoscape[38] to construct a connection map for the gene regulatory network, as shown in Supplementary Fig. 6. The thickness of line connecting TFs and target genes represented the weight of regulatory link predicted by SCENIC.

Cytokine/receptor interaction analysis

To identify potential cellular communications between monocytes and other cell types ($CD4^+$ T, $CD8^+$ T, B, plasma B and NK cells), we applied the CellphoneDB[26] algorithm to the scRNA-seq profiles from the the severe and remission stages, and in healthy control individuals. CellphoneDB evaluated the impact of a ligand/receptor interactions based on the ligand expression in one cell type and its corresponding receptor expression in another cell type. We focused on the enriched cytokine/receptor interactions in severe-stage COVID-19 patients, and selected the cytokine/receptor interactions with more significant (*P* value < 0.05) cell-cell interaction pairs in the severe stage than that in the remission and healthy stages. We also included cytokine/receptor pairs which were highly expressed in severe stage.

Deconvolution of cell clusters from bulk RNA-seq data

We applied AutoGeneS[32] to deconvolute the composition of cell clusters based on the signature genes identified in our single-cell analysis. Specifically, we first obtained a gene-by-cluster expression matrix from our normalized single-cell profile, where the matrix elements were the average expression of each gene in each cell cluster. We then defined the top 5000 most variable genes between cell cluster and the 2000 DEGs used for cell clustering as the "VarGenes", and extracted the VarGenes-by-cluster expression matrix as the feature gene expression profile for AutoGeneS. We set the input parameters as "model = 'nusvr', ngen = 1000, seed = 0, nfeatures = 1500" to deconvolute the cell composition in AutoGeneS.

Statistical analysis

The two-tailed Wilcoxon rank-sum test (also called the Mann-Whitney U test) was used to search for the DEGs and to compare the expression differences of a gene set of interest between two conditions. In CellphoneDB, a permutation test was used to evaluate the significance of a cytokine/receptor pair. Metascape utilizes the hypergeometric test and Benjamini-Hochberg *P* value correction algorithm to identify the ontology terms that contain a statistically greater number of genes in common than expected. We used the Student's t-test to evaluate the significance of the expression differences of the TFs (and their target genes) between samples from severe stage patients and healthy controls.

Data Availability

The scRNA-seq data of PBMCs from the 2 severe COVID-19 patients can be obtained from the Genome Sequence Archive (GSA) at BIG Data Center and the accession number is CRA002509. We also used published datasets as controls or comparable data, including (1) the scRNA-seq data of PBMCs from 2 healthy donors

downloaded from the 10X genomics official website https://support.10xgenomics.com/single-cell-gene-expression/datasets/3.1.0/5k_pbmc_NGSC3_aggr, (2) the scRNA-seq data of PBMCs from 22 sepsis patients and 19 related controls[25] that is available on Institute Single Cell Portal (https://singlecell.broadinstitute.org/single_cell) with accesson number SCP548, (3) the bulk RNA-seq data of PBMCs from 3 COVID-19 patients and 3 related controls[31] downloaded from the GSA at BIG Data Center with accession number CRA002390.

Code Availability

Analysis scripts are accessible from github: https://github.com/QuKunLab/COVID-19.

References:

1. WHO. Coronavirus disease 2019 (COVID-19) Situation Report - 102. (2020).

2. Wu Z, McGoogan JM. Characteristics of and Important Lessons From the Coronavirus Disease 2019 (COVID-19) Outbreak in China: Summary of a Report of 72314 Cases From the Chinese Center for Disease Control and Prevention. *JAMA*, (2020).

3. Mehta P, *et al.* COVID-19: consider cytokine storm syndromes and immunosuppression. *Lancet* **395**, 1033-1034 (2020).

4. Zhou Y, *et al.* Pathogenic T cells and inflammatory monocytes incite inflammatory storm in severe COVID-19 patients. *National Science Review*, (2020).

5. Zumla A, Hui DS, Azhar EI, Memish ZA, Maeurer M. Reducing mortality from 2019-nCoV: host-directed therapies should be an option. *Lancet* **395**, e35-e36 (2020).

6. Chaofu Wang JX, Lei Zhao et al. Aveolar Macrophage Activation and Cytokine Storm in the Pathogenesis of Severe COVID-19. *PREPRINT (Version 1) available at Research Square*

[+https://doiorg/1021203/rs3rs-19346/v1+], (2020).

7. Li G, *et al.* Coronavirus infections and immune responses. *J Med Virol* **92**, 424-432 (2020).

8. Huang C, *et al.* Clinical features of patients infected with 2019 novel coronavirus in Wuhan, China. *Lancet* **395**, 497-506 (2020).

9. Cao X. COVID-19: immunopathology and its implications for therapy. *Nat Rev Immunol* **20**, 269-270 (2020).

10. Moore JB, June CH. Cytokine release syndrome in severe COVID-19. *Science* **368**, 473-474 (2020).

11. Kotch C, Barrett D, Teachey DT. Tocilizumab for the treatment of chimeric antigen receptor T cell-induced cytokine release syndrome. *Expert Rev Clin Immunol* **15**, 813-822 (2019).

12. Le RQ, *et al.* FDA Approval Summary: Tocilizumab for Treatment of Chimeric Antigen Receptor T Cell-Induced Severe or Life-Threatening Cytokine Release Syndrome. *Oncologist* **23**, 943-947 (2018).

13. Xu X, *et al.* Effective treatment of severe COVID-19 patients with tocilizumab. *Proc Natl Acad Sci U S A*, 202005615 (2020).

14. Wolock SL, Lopez R, Klein AM. Scrublet: Computational Identification of Cell Doublets in Single-Cell Transcriptomic Data. *Cell Syst* **8**, 281-291 e289 (2019).

15. Butler A, Hoffman P, Smibert P, Papalexi E, Satija R. Integrating single-cell transcriptomic data across different conditions, technologies, and species. *Nat Biotechnol* **36**, 411-420 (2018).

16. Zheng GX, *et al.* Massively parallel digital transcriptional profiling of single cells. *Nat Commun* **8**, 14049 (2017).

17. Korsunsky I, *et al.* Fast, sensitive and accurate integration of single-cell data with Harmony. *Nat Methods*, (2019).

18. Norelli M, *et al.* Monocyte-derived IL-1 and IL-6 are differentially required for cytokine-release syndrome and neurotoxicity due to CAR T cells. *Nat Med* **24**, 739-748 (2018).

19. Aibar S, *et al.* SCENIC: single-cell regulatory network inference and clustering. *Nat Methods* **14**, 1083-1086 (2017).

20. Liu Q, Zhou YH, Yang ZQ. The cytokine storm of severe influenza and development of immunomodulatory therapy. *Cellular & Molecular Immunology* **13**, 3-10 (2016).

21. Tisoncik JR, Korth MJ, Simmons CP, Farrar J, Martin TR, Katze MG. Into the Eye of the Cytokine Storm. *Microbiol Mol Biol R* **76**, 16-32 (2012).

22. Bhatraju PK, *et al.* Covid-19 in Critically Ill Patients in the Seattle Region - Case Series. *N Engl J Med*, (2020).

23. Arentz M, *et al.* Characteristics and Outcomes of 21 Critically Ill Patients With COVID-19 in Washington State. *JAMA*, (2020).

24. Guo T, *et al.* Cardiovascular Implications of Fatal Outcomes of Patients With Coronavirus Disease 2019 (COVID-19). *JAMA Cardiol*, (2020).

25. Reyes M, *et al.* An immune-cell signature of bacterial sepsis. *Nat Med*, (2020).

26. Vento-Tormo R, *et al.* Single-cell reconstruction of the early maternal-fetal interface in humans. *Nature* **563**, 347-353 (2018).

27. Guan W, *et al.* Clinical Correlations of Transcriptional Profile in Patients Infected With Avian Influenza H7N9 Virus. *J Infect Dis* **218**, 1238-1248 (2018).

28. Wang Z, *et al.* Recovery from severe H7N9 disease is associated with diverse response mechanisms dominated by CD8(+) T cells. *Nat Commun* **6**, 6833 (2015).

29. Thevarajan I, *et al.* Breadth of concomitant immune responses prior to patient recovery: a case report of non-severe COVID-19. *Nature Medicine*, (2020).

30. Harty JT, Tvinnereim AR, White DW. CD8+ T cell effector mechanisms in resistance to infection. *Annu Rev Immunol* **18**, 275-308 (2000).

31. Xiong Y, *et al.* Transcriptomic characteristics of bronchoalveolar lavage fluid and peripheral blood mononuclear cells in COVID-19 patients. *Emerg*

Microbes Infect **9**, 761-770 (2020).

32. Aliee H, Theis F. AutoGeneS: Automatic gene selection using multi-objective optimization for RNA-seq deconvolution. *BioRxiv*, 2020.2002.2021.940650 (2020).

33. Braciale TJ, Sun J, Kim TS. Regulating the adaptive immune response to respiratory virus infection. *Nat Rev Immunol* **12**, 295-305 (2012).

34. Rouse BT, Sehrawat S. Immunity and immunopathology to viruses: what decides the outcome? *Nat Rev Immunol* **10**, 514-526 (2010).

35. Ahn SS, Jung SM, Song JJ, Park YB, Park JY, Lee SW. Safety of Tocilizumab in Rheumatoid Arthritis Patients with Resolved Hepatitis B Virus Infection: Data from Real-World Experience. *Yonsei Med J* **59**, 452-456 (2018).

36. Bersanelli M. Controversies about COVID-19 and anticancer treatment with immune checkpoint inhibitors. *Immunotherapy*, (2020).

37. Zhou Y, *et al.* Metascape provides a biologist-oriented resource for the analysis of systems-level datasets. *Nat Commun* **10**, 1523 (2019).

38. Cline MS, *et al.* Integration of biological networks and gene expression data using Cytoscape. *Nat Protoc* **2**, 2366-2382 (2007).

Acknowledgements

Funding: This work was supported by the National Key R&D Program of China (2017YFA0102900 to K.Q.), the National Natural Science Foundation of China grants (91940306, 81788101, 31970858, 31771428 and 91640113 to K.Q., 31700796 to C.G. and 81871479 to J.L.), the Fundamental Research Funds for the Central Universities (to K.Q.). We thank the USTC supercomputing center and the School of Life Science Bioinformatics Center for providing supercomputing resources for this project. We thank the CAS interdisciplinary innovation team for helpful discussion.

Author Contributions

669 K.Q. conceived and supervised the project; K.Q., C.G. and J.L. designed the
670 experiments; C.G. and J.L. performed the experiments and conducted all the sample
671 preparation for next-generation sequencing with the help from H.M. and T.C.; B.L.
672 performed the data analysis with the help from P.C., Q.Y., L.Z., L.J., C.J., Q.L., D.Z.,
673 W.Z., Y.L., K.L., X.G. and J.F.; T.C., X.W., L.L., J.W. and X.M. provided
674 COVID-19 blood samples and clinical information; J.W. contributed to the revision of
675 the manuscript; K.Q., C.G., J.L. and B.L. wrote the manuscript with the help of B.F.,
676 H.W. and all the other authors.
677
678 **Competing interests**
679 Jingwen Fang is the chief executive officer of HanGen Biotech.
680
681 **Figure Legends**
682
683 **Figure 1 | An atlas of peripheral immune cells in severe COVID-19 patients. a**,
684 Flowchart depicting the overall design of the study. Blood draws from patient P1 were
685 performed at 2 time points (day 1 and day 5), and from P2 at 3 time points (day 1, day
686 5 and day 7). P1 at day 1 and P2 at day 1 and day 5 were positive for the nucleic acid
687 test of a throat swab specimen. P1 at day 5 and P2 at day 7 were negative for the
688 nucleic acid test of a throat swab specimen. Patients at day 1 were at the severe stage,
689 were in the remission stage at day 5 (P1 and P2); the day 7 blood draw for P2 (still
690 remission stage) was based on a positive nucleic acid test at day 5. Note that samples
691 on day 1 were collected within 12 hours of Tocilizumab treatment. **b-d**, UMAP
692 representations of integrated single-cell transcriptomes of 69,237 PBMCs, with
693 13,239 cells from our COVID-19 patients and 55,998 were from 10X official
694 website[16]. Cells are color-coded by clusters **(b)**, disease state **(c)**, and sample origin
695 **(d)**. Dotted circles represented cell types with > 5% proportion of PBMCs in **(b)**, and
696 clusters significantly enriched in patients versus controls in **(c, d)**. Mono, monocyte;
697 NK, natural killer cells; mDC, myeloid dendritic cells; pDC, plasmacytoid dendritic

cells. **e**, Violin plots of selected marker genes (upper row) for multiple cell subpopulations. The left column presents the cell subtypes as identified based on combinations of marker genes.

Figure 2 | A unique monocyte subpopulation contributes to the inflammatory storm in severe-stage COVID-19 patients. a, UMAP plot showing 3 clusters of $CD14^+$ monocytes and 1 cluster of $CD16^+$ monocyte. Cells are color-coded by clusters. **b**, Bar plot of the proportion of monocytes in cluster 9 at the severe and remission stages, and in healthy control individuals. **c**, Heatmap of differentially expressed genes (DEGs) in monocytes from pairwise comparison between the severe stage patients, remission stage patients, and healthy control individuals. **d**, UMAP plots showing the expression of selected cytokines in all monocyte clusters. **e,f,** Box plot of the average expression of genes involved in the signaling pathway " Regulation of acute inflammatory response " and "Cell chemotaxis" in monocytes from the severe and remission stages, and in healthy control individuals. Center line, median; box limits, upper and lower quartiles; whiskers, 1.5x interquartile range; points, outliers; **** represents *P* value < 10^{-100}, Wilcoxon rank-sum test. **g**, Heatmap of the area under the curve (AUC) scores of expression regulation by transcription factors (TFs), as estimated using SCENIC. Shown are the top-ranked TFs having the highest difference in expression regulation estimates in monocytes from severe-stage COVID-19 patients. **h**, UMAP plots showing the expression of the *ATF3*, *NFIL3*, and *HIVEP2* genes in monocytes (top) and the AUC of the estimated regulon activity of the corresponding TFs, predicting the degree of expression regulation of their target genes (bottom).

Figure 3 | The monocyte-centric molecular interactions of peripheral immune cells in severe-stage COVID-19 patients. a, Dot plot of predicted interactions between monocytes and the indicated immune cell types in the severe and remission

726 stages, and in healthy control individuals. *P* values were measured by circle sizes,
727 scale on right (permutation test). The means of the average expression level of
728 interacting molecule 1 in cluster 1 and interacting molecule 2 in cluster 2 are
729 indicated by color. Assays were carried out at the mRNA level, but are extrapolated to
730 protein interactions. **b**, Summary illustration depicting the potential cytokine/receptor
731 interactions between monocytes and other types of peripheral immune cells in the
732 severe and remission stages, and in healthy control individuals. Bolder lines indicate
733 predicted enriched cytokine/receptor interactions between monocytes and other
734 immune cell types.
735
736 **Figure 4 | Enhanced humoral and cell-mediated immunity in severe COVID-19**
737 **patients. a**, UMAP representations of B and plasma B cell clusters from the severe
738 and remission stages, and in healthy control individuals. **b**, Bar plot of the proportions
739 of plasma B cells in the B cell lineage from the severe and remission stages, and in
740 healthy control individuals. **c**, UMAP representations of $CD8^+$ T cell subtypes (left)
741 and the distribution of cells from the severe and remission stages, and in healthy
742 control individuals in each subtype (right). **d**, Dot plot of the expression of the *CCR7*,
743 *PRDM1*, and *MKI67* genes in all $CD8^+$ T cell subtypes. **e**, Heatmap of differentially
744 expressed genes in effector $CD8^+$ T cells from pairwise comparisons between the
745 severe stage patients, remission stage patients, and healthy control individuals. **f, g,**
746 Bar plots of GO terms enriched in effector $CD8^+$ T cells from the severe stage **(f)** or
747 the severe and remission stages **(g)**. **h, i,** Box plots of the average expression of genes
748 "cell chemotaxis" and "regulation of cell killing" in the effector $CD8^+$ T cells from
749 severe stage, remission stage, and healthy controls. Center line, median; box limits,
750 upper and lower quartiles; whiskers, 1.5x interquartile range; points, outliers; ****
751 represents *P* value < 10^{-30}. Wilcoxon rank-sum test.
752
753 **Supplementary Figure Legends and Supplementary Tables**

Supplementary Figure 1 | Quality control of single-cell data for PBMC samples from severe COVID-19 patients. a, Summary of captured cells, median genes per cell, median UMIs per cell, and the number of cells that passed quality control (QC) in distinct batches of single-cell data from severe COVID-19 patients. **b-d,** Box plots showing the gene number **(b)**, UMI number **(c)**, and percentage of mitochondrial RNA **(d)** in distinct batches of single-cell data from severe COVID-19 patients. **e, f,** Aggregated scRNA-seq one-to-one reproducibility plots for technical replicates **(e)** and biological replicates **(f)**. The correlation (R) represents the Pearson correlation across all genes. Box-whisker plot; the lower whisker is the lowest value greater than the 25% quantile minus 1.5 times the interquartile range (IQR), the lower hinge is the 25% quantile, the middle is the median, the upper hinge is the 75% quantile and the upper whisker is the largest value less than the 75% quantile plus 1.5 times the IQR.

Supplementary Figure 2 | Single-cell transcriptomes of PBMCs from patient P1 or P2 at each time point. a, UMAP plot showing single-cell transcriptomes from patient P1 and P2 at day 1. **b,** UMAP plot showing single-cell transcriptomes from patient P1 at day 5 and P2 at day 5 and day 7.

Supplementary Figure 3 | Single-cell profiling of peripheral immune cells in severe COVID-19 integrated with healthy controls using Harmony. a, UMAP representations of single-cell transcriptomes of 69,237 PBMCs integrated by Harmony. Cells are color-coded by clusters and disease state (see legend for key). Mono, monocyte; NK, natural killer cells; mDC, myeloid dendritic cells; pDC, plasmacytoid dendritic cells. **b,** Violin plots of selected marker genes (upper row) for multiple cell subpopulations. The left column presents the cell subtypes as identified based on combinations of marker genes. **c**, Jaccard similarities between the cell clusters with the integration processed by Seurat (version 3.1.4) and with the

integration processed by Harmony.

Supplementary Figure 4 | The composition of cell clusters identified in the integrated single-cell transcriptomes of PBMCs from the severe and remission stages, and in healthy control individuals. a, Bar chart showing the percentage of cell clusters in the severe and remission stages, and in healthy controls. **b**, Pie chart showing the proportion of cells from each disease state in selected cell clusters (cluster 2, 13, 10, 15), which were present in remission-stage patients and in healthy controls, but not in severe-stage patients. **c**, Pie chart showing the proportion of cells from each disease state in selected cell clusters (cluster 9, 6, 12, 11), which were present in severe and remission stages but not in healthy controls.

Supplementary Figure 5 | GO terms enriched among DEGs highly expressed in monocyte at the severe stage or at severe and remission stages. a, b, Bar plots of enriched GO terms of genes highly expressed in monocytes at the severe stage **(a)** or at the severe and remission stages **(b)**.

Supplementary Figure 6 | Severe-stage-specific monocyte regulatory network predicted by SCENIC. Transcription factors are shown as rectangles; their target genes are shown as circles. Student's t-test.

Supplementary Figure 7 | Integrated single-cell transcriptome analysis from patients with sepsis and our COVID-19 patients. a, b, UMAP representations of integrated single-cell transcriptomes from patients with sepsis at mild stage (Int-URO, n = 7)[25], patients with sepsis at severe stage (ICU-SEP, n = 8)[25], critically ill patients without sepsis (ICU-NoSEP, n = 7)[25], healthy controls from outside our study (Control, n = 19)[25], and our COVID-19 patients (Severe COVID-19 and remission COVID-19). Cells are color-coded by clusters **(a)**, disease states **(b)**. **c**, Bar chart

showing the proportion of cell clusters in (**a**) in each disease state.

Supplementary Figure 8 | The composition of cell clusters identified in our single-cell analysis in a bulk RNA-seq from three severe COVID-19 patients and healthy controls. a, Bar chart showing an estimation of the composition of each cell cluster of PBMCs deconvoluted from bulk RNA-seq data from three COVID-19 patients and healthy controls[31]. **b, c**, Bar chart showing the percentage of severe-stage-specific monocytes (cluster 9, **b**) and plasma B cells (cluster 11, **c**) in COVID-19 patients and healthy controls, deconvoluted from bulk RNA-seq. Student's t-test.

Supplementary Table 1 | Baseline characteristics and laboratory findings for the two COVID-19 patients in this study.

Supplementary Table 2 | Sequencing data quality.

Supplementary Table 3 | DEGs of different disease stages of the monocytes.

Supplementary Table 4 | GO terms enriched among DEGs in different disease stages of the monocytes.

Supplementary Table 5 | Sets of genes entailed in the enriched GO terms from Figure 2e and 2f.

Supplementary Table 6 | Interactions of cytokines and receptors in different disease stages, predicted using CellphoneDB.

Supplementary Table 7 | Drugs targeting cytokines or cytokine receptors.

Supplementary Table 8 | DEGs of different disease stages of effector $CD8^+$ T cells.

Supplementary Table 9 | GO terms enriched among DEGs in different disease stages of the effector $CD8^+$ T cells.

Supplementary Table 10 | Set of genes entailed in the enriched GO terms from Figure 4h and 4i.

838

839

Figure1

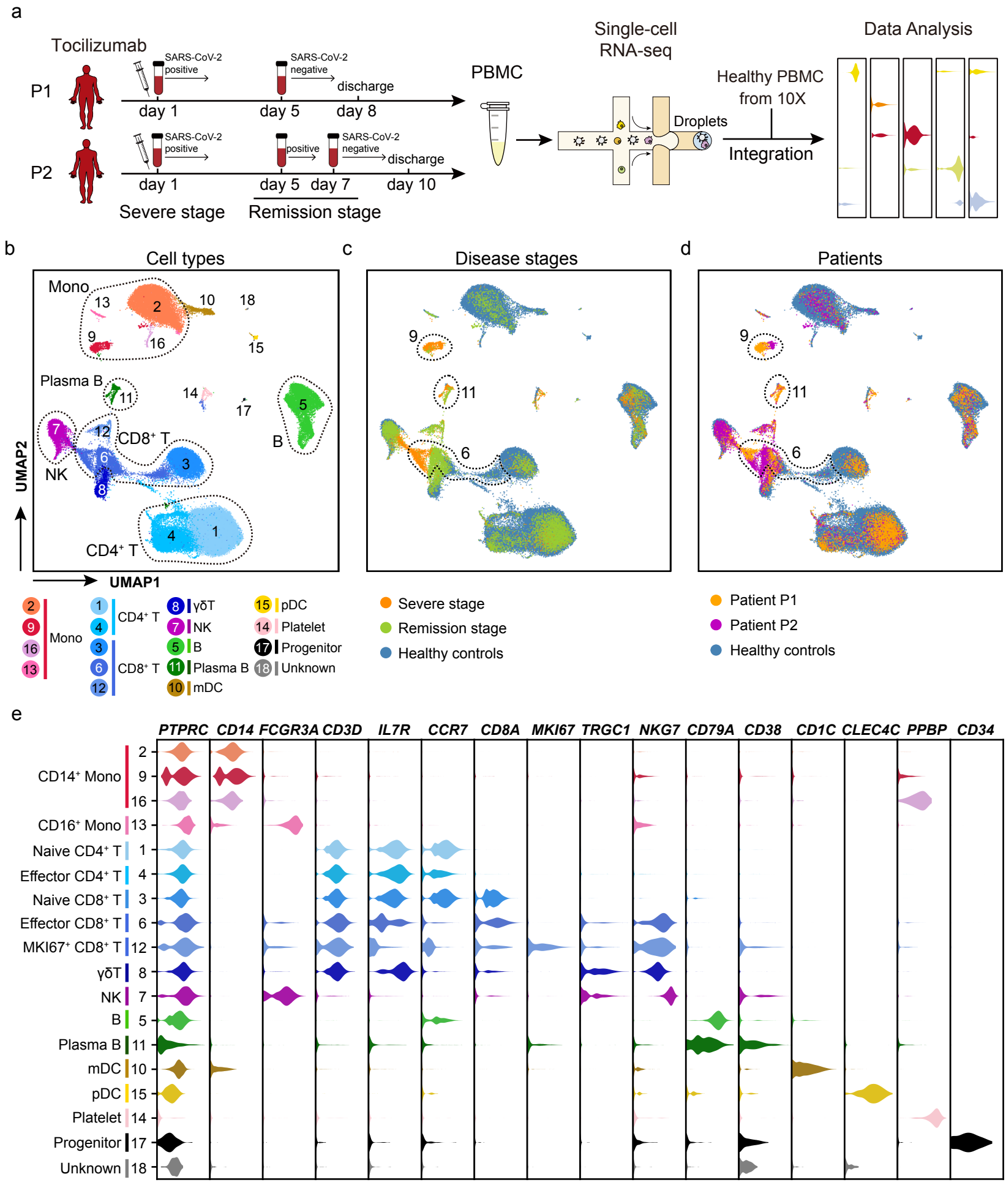
a
Tocilizumab
P1
P2
SARS-CoV-2 positive
SARS-CoV-2 negative
discharge
positive
day 1
day 5
day 7
day 8
day 10
Severe stage
Remission stage
PBMC
Single-cell RNA-seq
Droplets
Healthy PBMC from 10X
Integration
Data Analysis
b
Cell types
c
Disease stages
d
Patients
Mono
Plasma B
CD8⁺ T
NK
B
CD4⁺ T
UMAP2
UMAP1
Severe stage
Remission stage
Healthy controls
Patient P1
Patient P2
Healthy controls
Mono
CD4⁺ T
CD8⁺ T
γδT
NK
B
Plasma B
mDC
pDC
Platelet
Progenitor
Unknown
e
PTPRC
CD14
FCGR3A
CD3D
IL7R
CCR7
CD8A
MKI67
TRGC1
NKG7
CD79A
CD38
CD1C
CLEC4C
PPBP
CD34
CD14⁺ Mono
CD16⁺ Mono
Naive CD4⁺ T
Effector CD4⁺ T
Naive CD8⁺ T
Effector CD8⁺ T
MKI67⁺ CD8⁺ T
γδT
NK
B
Plasma B
mDC
pDC
Platelet
Progenitor
Unknown

Figure2

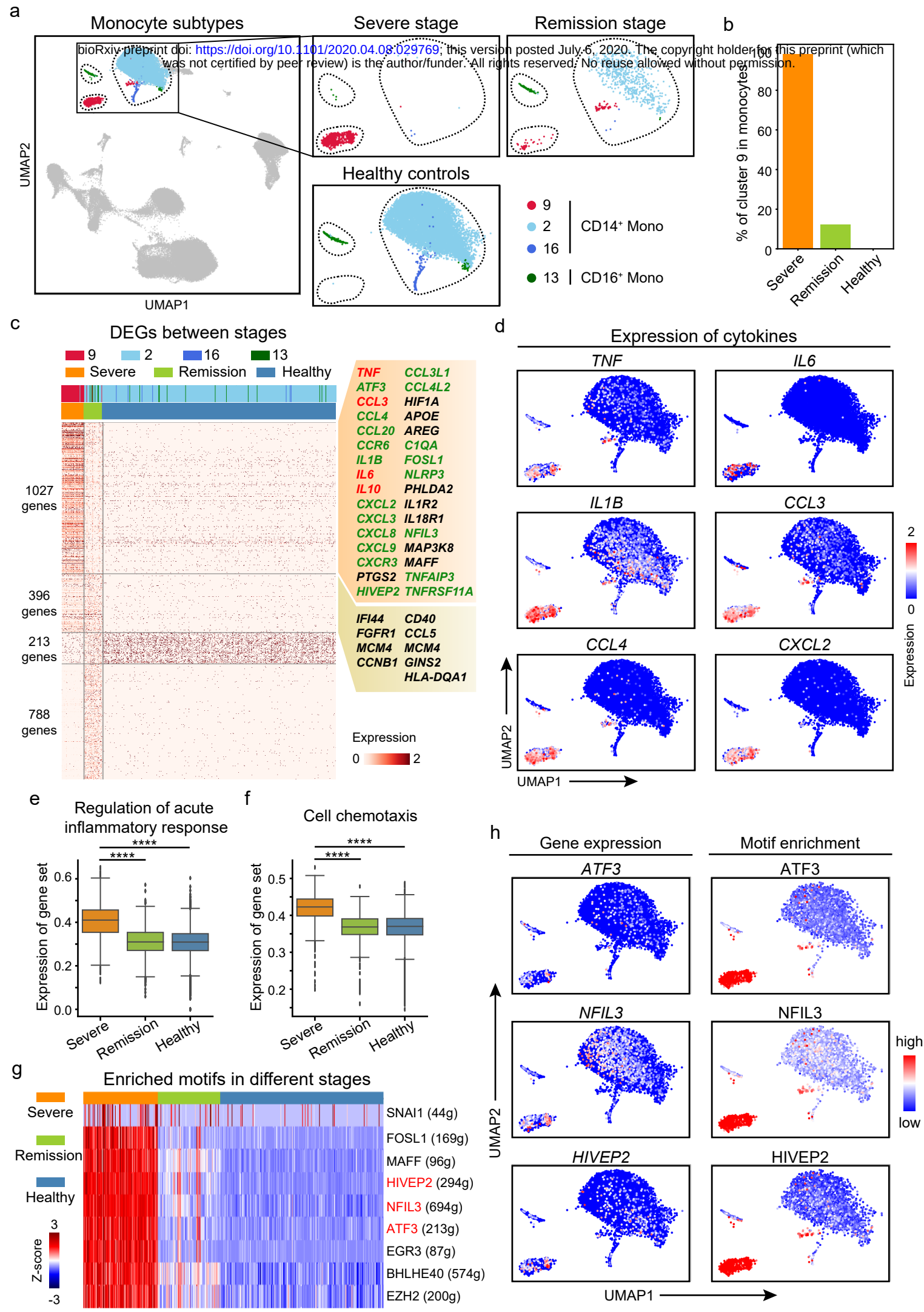

Figure3

a

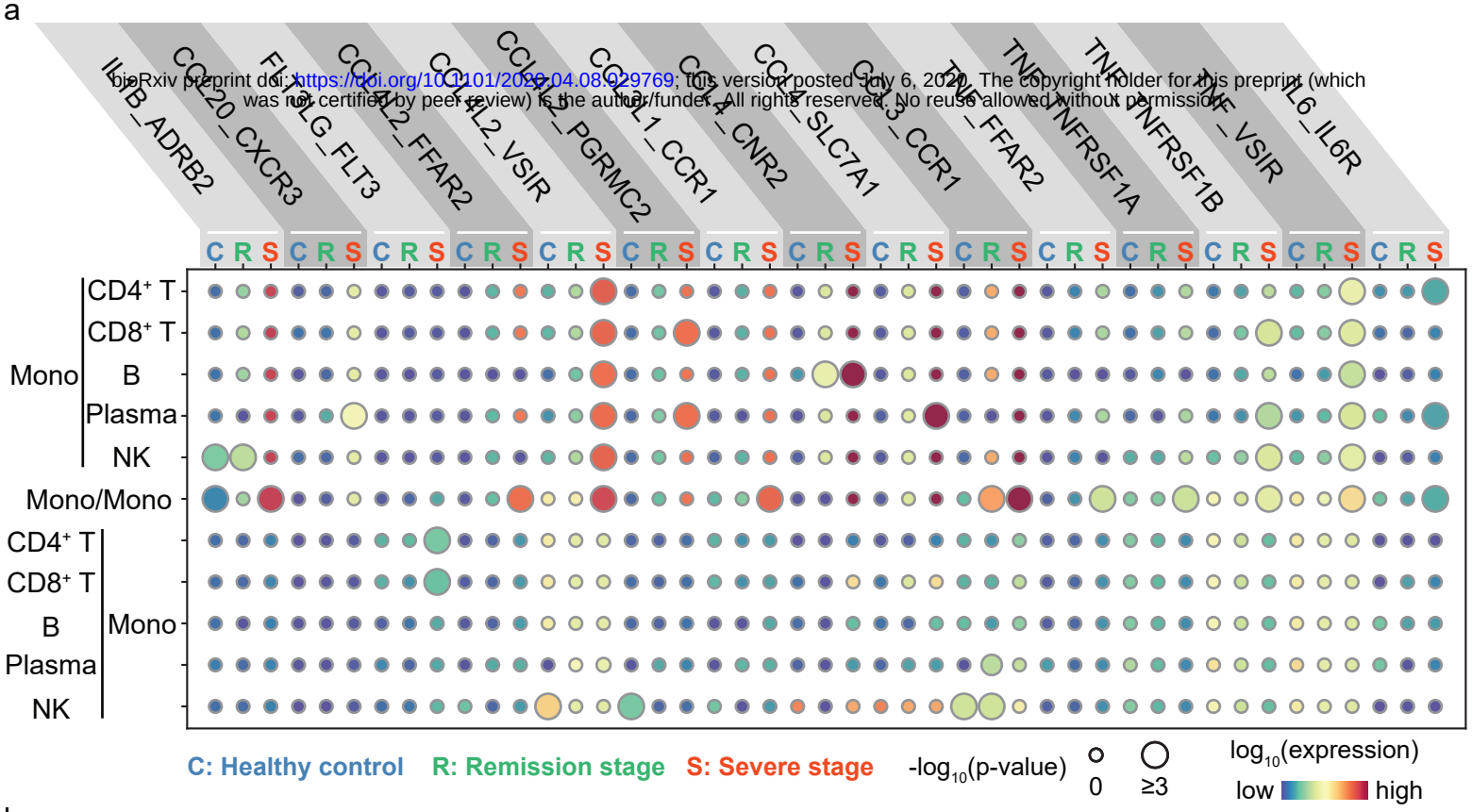

b

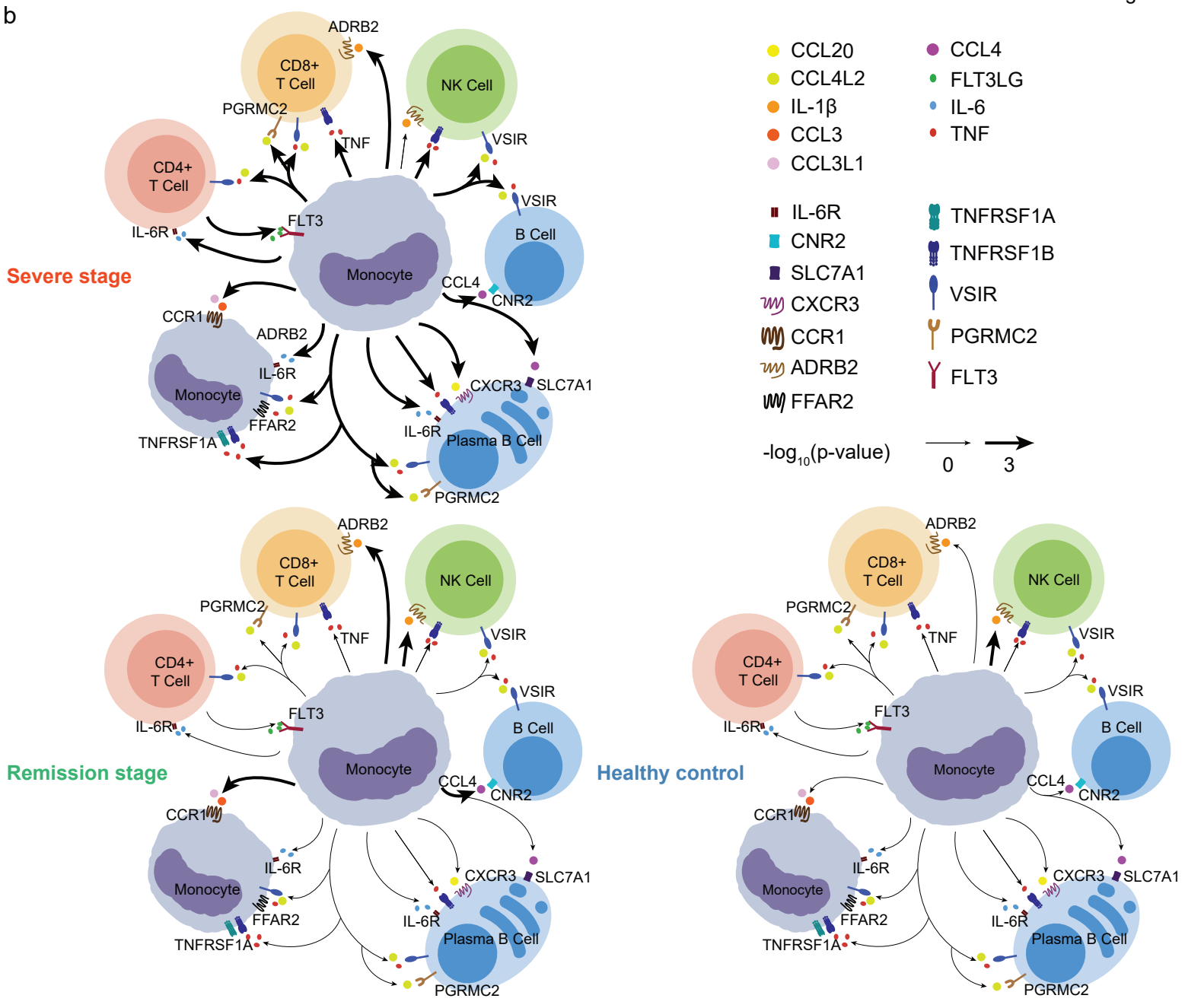

Figure4

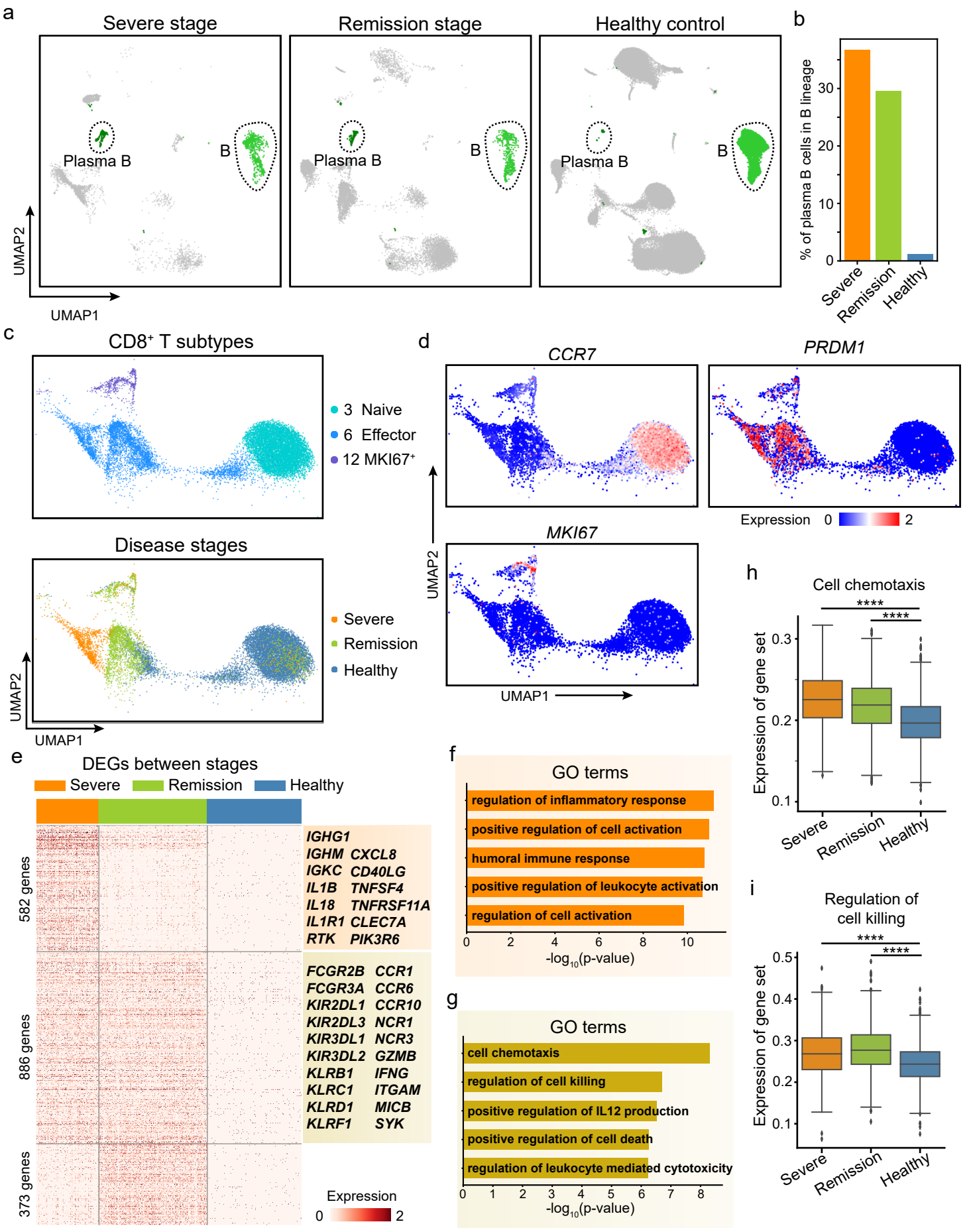
a
Severe stage
Remission stage
Healthy control
Plasma B
B
UMAP2
UMAP1
b
% of plasma B cells in B lineage
0
10
20
30
Severe
Remission
Healthy
c
CD8⁺ T subtypes
3 Naive
6 Effector
12 MKI67⁺
Disease stages
Severe
Remission
Healthy
UMAP2
UMAP1
d
CCR7
PRDM1
MKI67
Expression 0 2
UMAP2
UMAP1
e
DEGs between stages
Severe
Remission
Healthy
582 genes
886 genes
373 genes
IGHG1
IGHM CXCL8
IGKC CD40LG
IL1B TNFSF4
IL18 TNFRSF11A
IL1R1 CLEC7A
RTK PIK3R6
FCGR2B CCR1
FCGR3A CCR6
KIR2DL1 CCR10
KIR2DL3 NCR1
KIR3DL1 NCR3
KIR3DL2 GZMB
KLRB1 IFNG
KLRC1 ITGAM
KLRD1 MICB
KLRF1 SYK
Expression
0
2
f
GO terms
regulation of inflammatory response
positive regulation of cell activation
humoral immune response
positive regulation of leukocyte activation
regulation of cell activation
0
2
4
6
8
10
-log10(p-value)
g
GO terms
cell chemotaxis
regulation of cell killing
positive regulation of IL12 production
positive regulation of cell death
regulation of leukocyte mediated cytotoxicity
0
1
2
3
4
5
6
7
8
-log10(p-value)
h
Cell chemotaxis
****
****
Expression of gene set
0.1
0.2
0.3
Severe
Remission
Healthy
i
Regulation of cell killing
****
****
Expression of gene set
0.1
0.2
0.3
0.4
0.5
Severe
Remission
Healthy

Supplementary Fig. 1

a

Batch name	Captured cells	Median genes per cell	Median UMIs per cell	Cells passed QC
P1-day1-rep1	2591	840	2068	1511
P1-day1-rep2	2081	862	2100	1257
P1-day5-rep1	3129	682	1850	2160
P1-day5-rep2	3851	691	1895	2699
P2-day1	2280	914	2067	1576
P2-day5	1488	810	1909	1027
P2-day7	3332	977	2238	3009

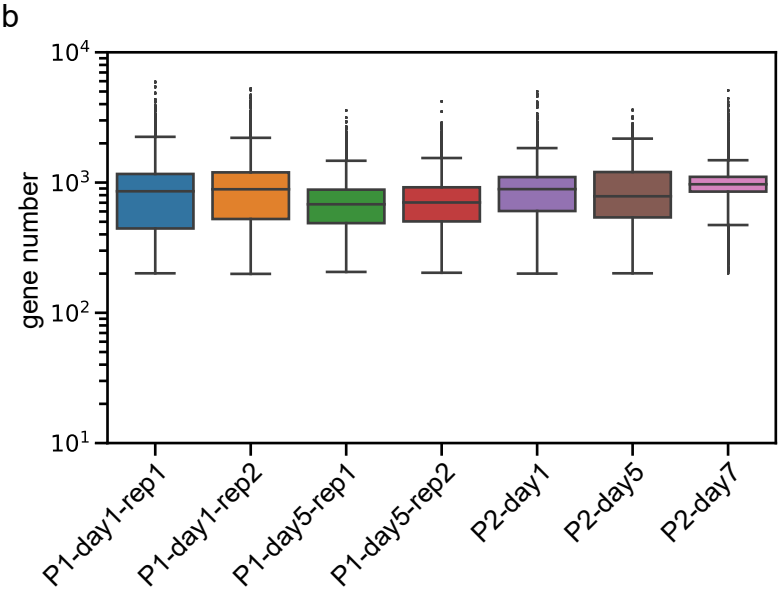

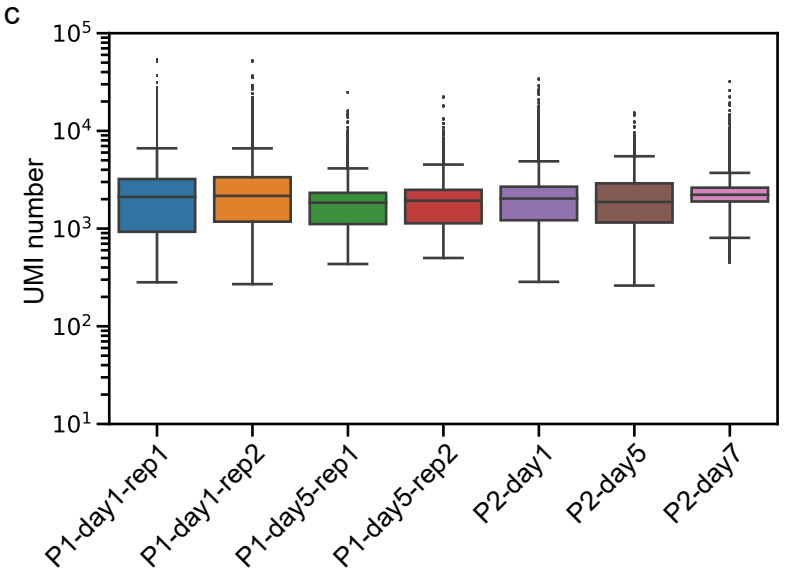

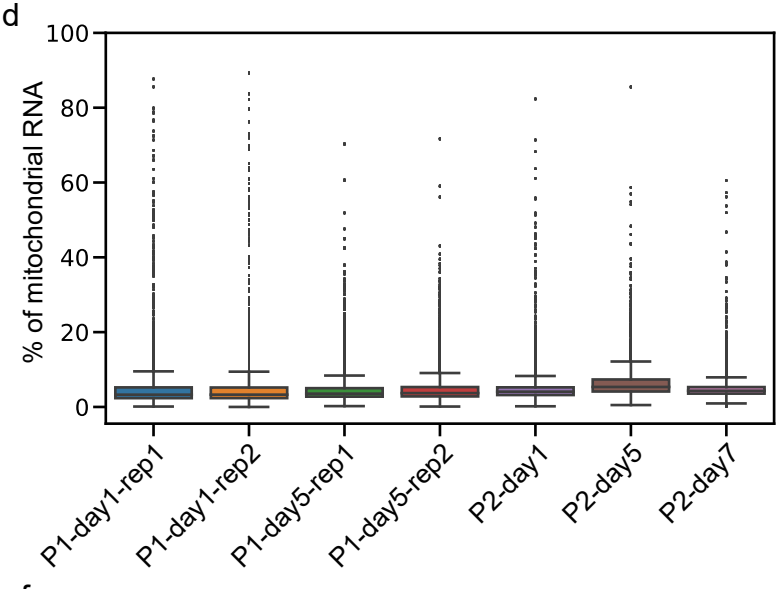

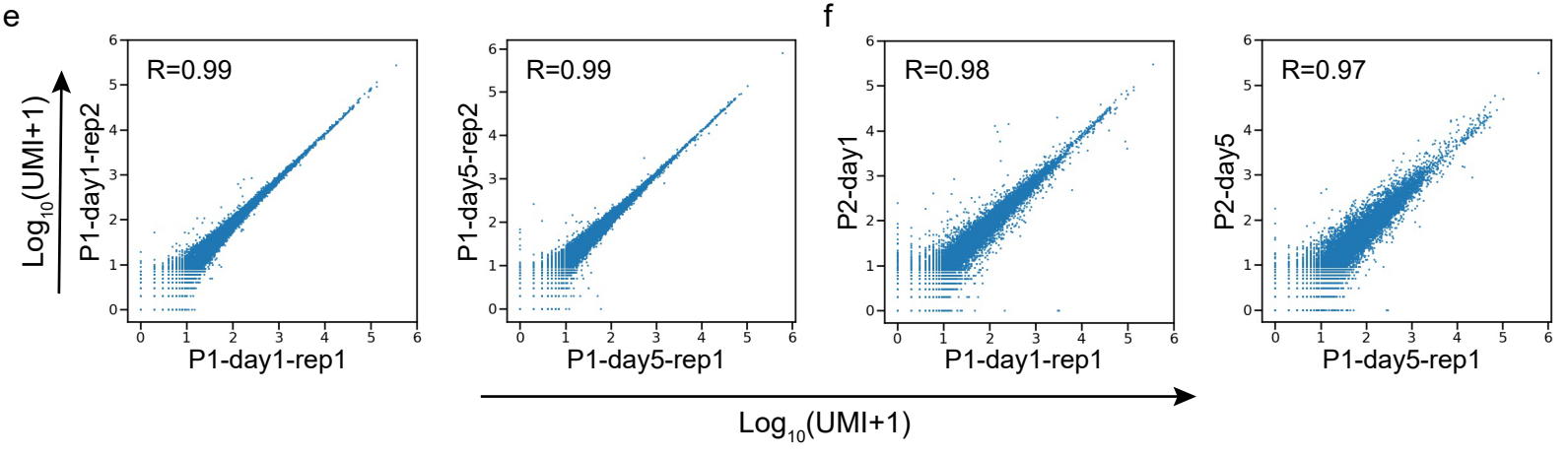

Supplementary Fig. 2

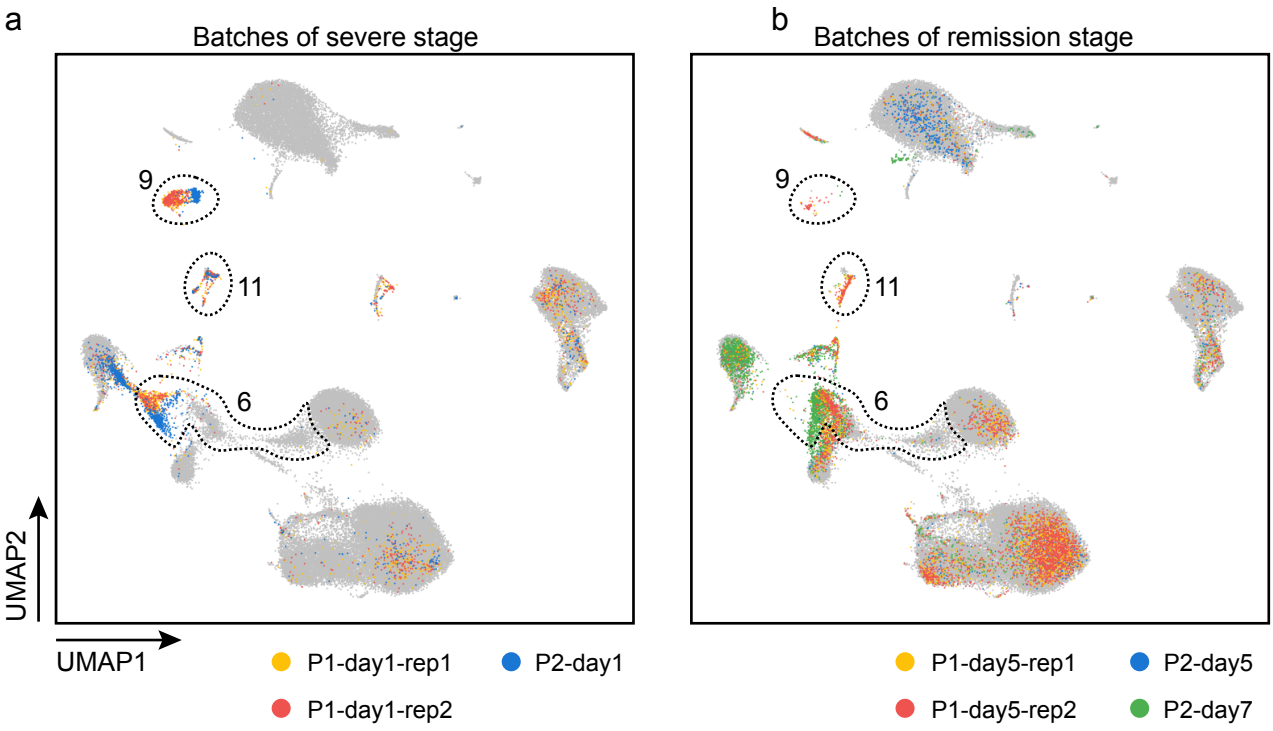

Supplementary Fig. 3

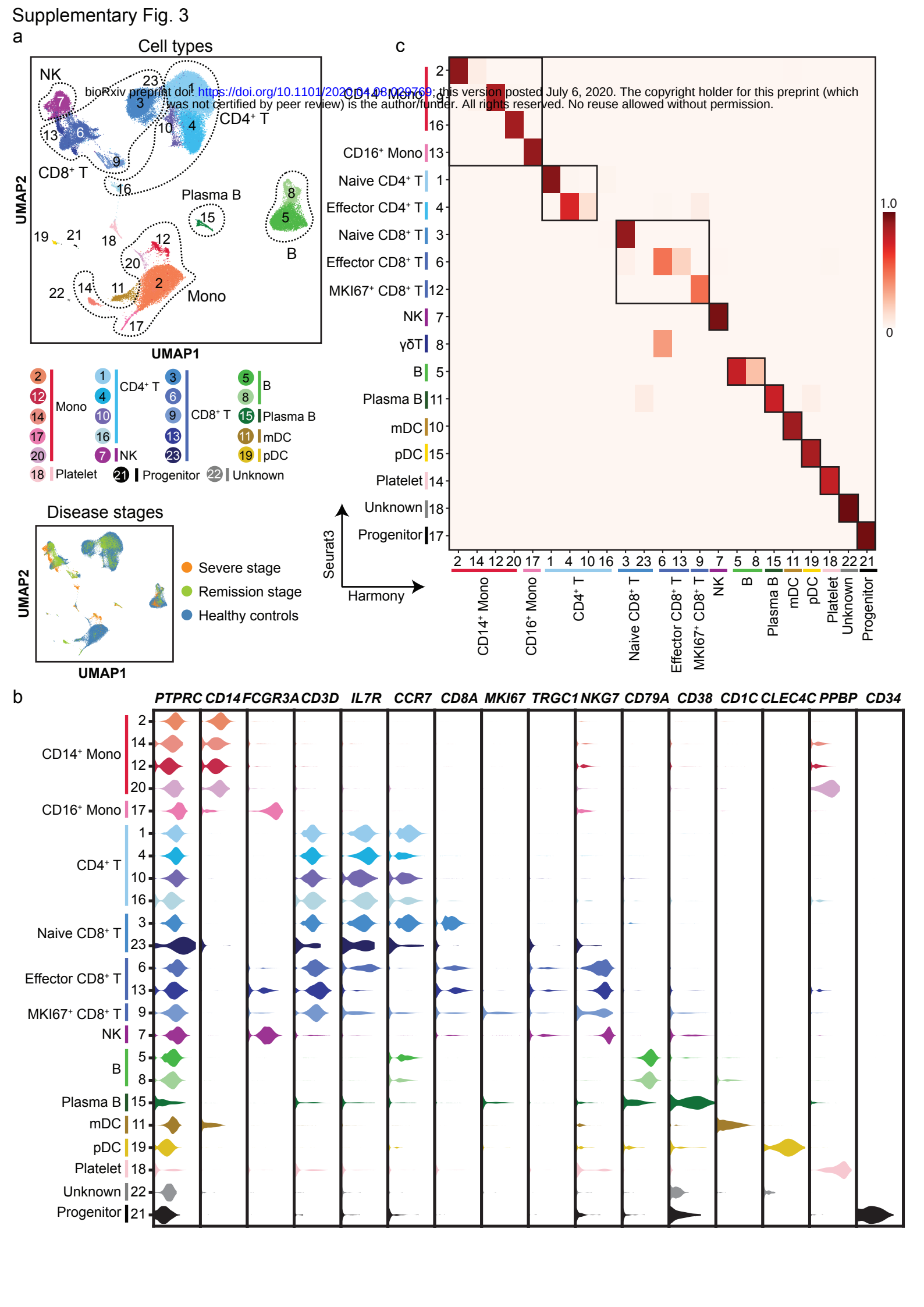

Supplementary Fig. 4

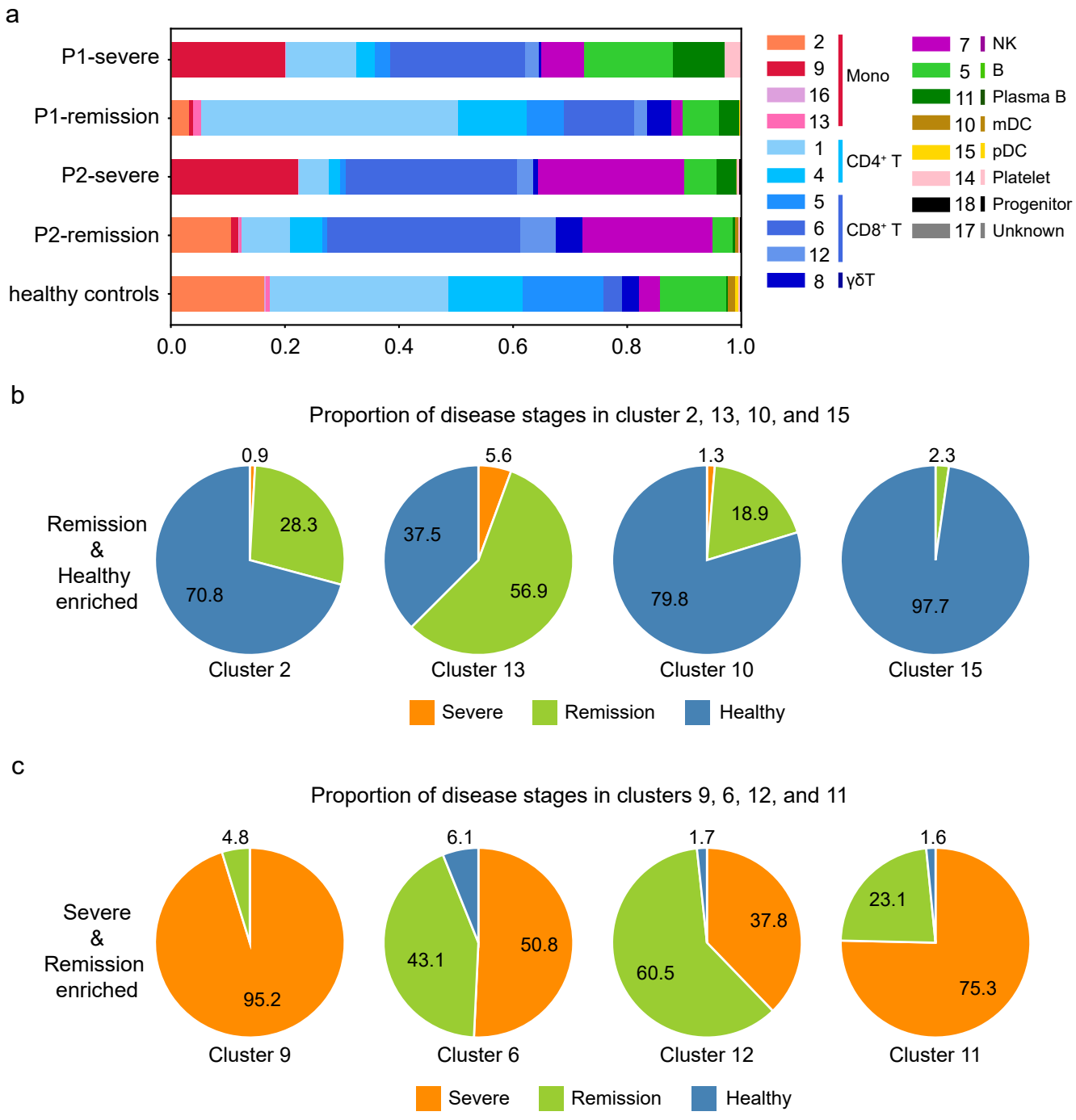

Supplementary Fig. 5

a

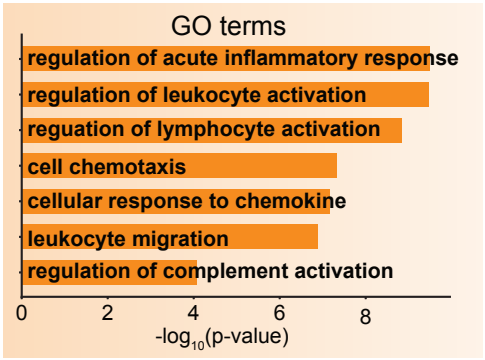

b

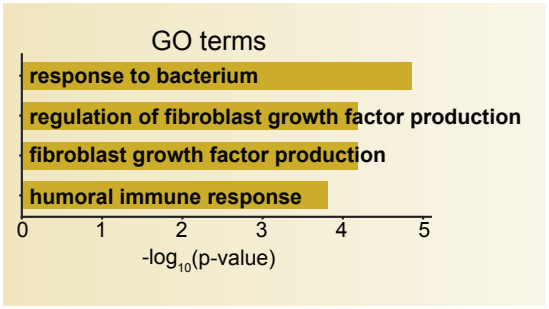

Supplementary Fig. 6

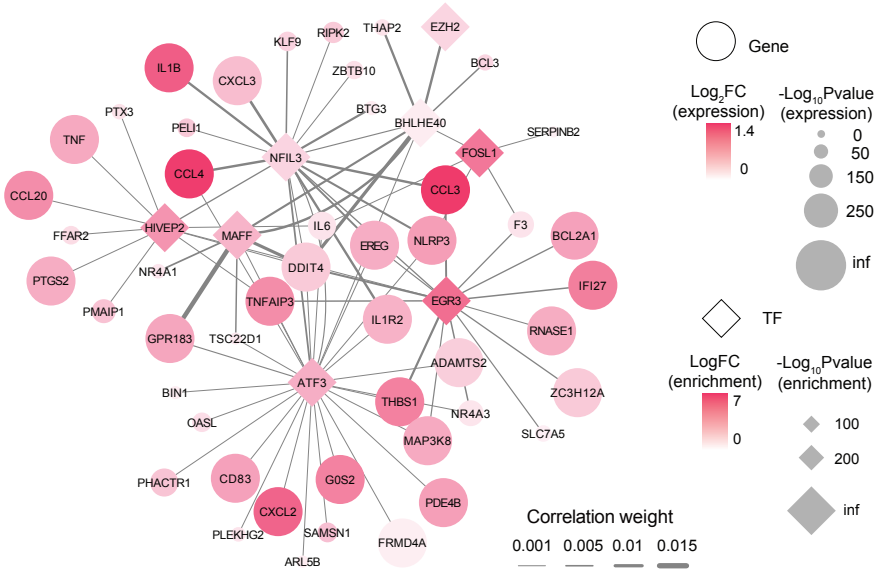

Supplementary Fig. 7

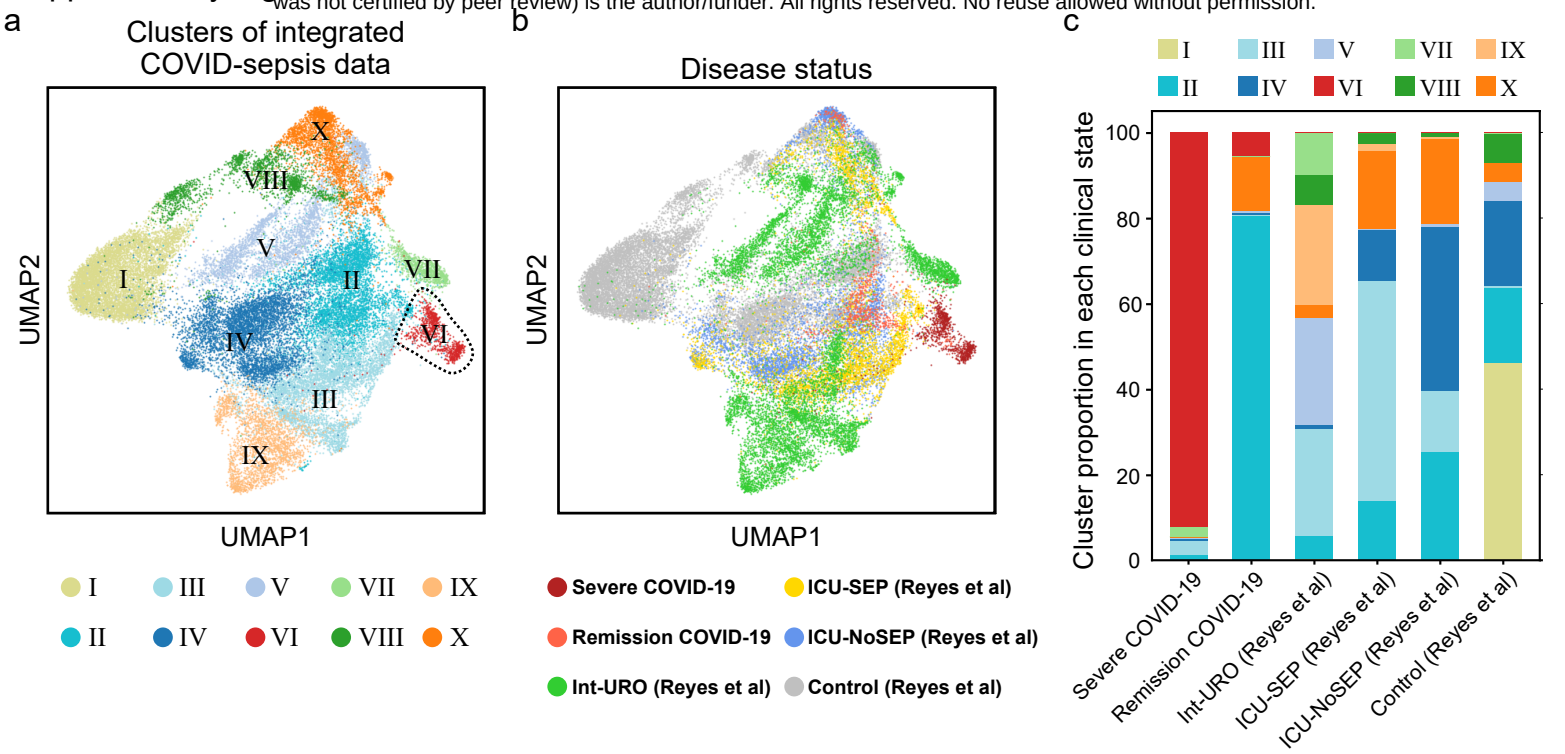

Supplementary Fig. 8